



Reprinted from JOURNAL OF THE ELECTROCHEMICAL SOCIETY  
Vol. 143, No. 6, June 1996  
Printed in U.S.A.  
Copyright 1996

# Electro-optical Charge Trapping in Zinc Porphyrin Films on Indium Tin Oxide and /SiO<sub>2</sub>/Si

Chong-yang Liu,<sup>a</sup> Turner Hasty,<sup>b</sup> and Allen J. Bard<sup>\*a</sup>

<sup>a</sup>Department of Chemistry and Biochemistry and <sup>b</sup>School of Engineering, The University of Texas at Austin, Austin, Texas 78712, USA

## ABSTRACT

A thin film of zinc octakis ( $\beta$ -octyloxyethyl) porphyrin (ZnOOEP) is capable of trapping and detrapping charge in an appropriate electric field under irradiation. An effective charge capacity of the order of  $30 \mu\text{C}/\text{cm}^2$  or  $10^{18}$  charges/ $\text{cm}^3$  was obtained with sandwich structures of ITO/ZnOOEP/ITO (where ITO is indium tin oxide) under a bias of 10 V with irradiation. Cells with the configuration ITO/ZnOOEP/SiO<sub>2</sub>/Si were also fabricated. When an electric field was applied across this cell in the dark, a small amount of charge was stored, as in a conventional capacitor. However, the charge stored under the same conditions with irradiation of the photoconductive ZnOOEP was three orders of magnitude higher. Trapped charge produced under illumination was not removed under short-circuit conditions in the dark, suggesting that this phenomenon could be used for information storage.

We recently described a data storage system based on single-layer sandwich cells containing thin films of the photoconductive material zinc octakis ( $\beta$ -decaoxyethyl) porphyrin (ZnODEP) deposited on the conductor indium tin oxide (ITO), in which electron-hole pairs were generated upon irradiation and separated under an electric field.<sup>1</sup> The movement of these separated charges is "frozen" by interrupting the irradiation because the dark conductivity of the film is low. Thus, information is stored as trapped charge. The data (charge) stored can be read as a voltage in the dark or as a photodischarge current. We demonstrated that the charge storage system is robust and non-volatile, with a response time for writing and reading in the nanosecond range and with no refreshing required for

long-term retention of trapped charge. By using a scanning tunneling microscope (STM) arrangement to apply a localized electric field, a memory density of at least 3 Gbits/ $\text{cm}^2$  was demonstrated. The number of charge-discharge cycles in the sandwich cells was over one billion.

In this report, we extend these studies to zinc octakis ( $\beta$ -octyloxyethyl) porphyrin (ZnOOEP), which has shorter hydrocarbon chains and shows a little higher photoconductivity than ZnODEP, and describe a new structure based on a Si/SiO<sub>2</sub> substrate. The use of these substrates demonstrates that it is possible to integrate these charge storage materials with Si to form hybrid structures that should be adaptable to well-developed silicon technology. Moreover, by adding a thin insulating layer of SiO<sub>2</sub>, thinner storage films of ZnOOEP can be used without dark self-discharge and with essentially total elimination of the

\* Electrochemical Society Fellow.

steady-state photocurrents found with ITO/ZnOOEP/ITO. An advantage of devices based on ZnOOEP or analogous films is that they show a much larger effective charge storage capacity ( $30 \mu\text{C}/\text{cm}^2$  or  $10^{18}/\text{cm}^3$ ) than those based on conventional dielectric materials<sup>2,3</sup> and thus are promising alternatives for ultrahigh density memory devices. The technical challenge is how to integrate such organic materials with conventional electronic materials and processing methods.

ZnOOEP may also find application in nonvolatile semiconductor memories, such as a floating gate device. In these devices, charges are forced by a high-voltage pulse to penetrate through the insulating layer (*i.e.*, avalanche injection) and are stored in the floating gate or at the insulator oxide interface of the metal/insulator/oxide/semiconductor (MIOS) system.<sup>4</sup> Such devices suffer inherently from a number of reliability problems, including high-voltage-induced degradation of the insulating layers, that severely limit the number of write/erase cycles.<sup>5</sup> The system described here, however, does not require a large potential bias in its operation, so a high stability is possible.

### Experimental

Three different cells, designated ITO/ZnOOEP/ITO, ITO/ZnOOEP/SiO<sub>2</sub>/Si, and ITO/ZnOOEP/silicone/Al, were prepared for these experiments. The first cell was prepared by capillary filling as described previously.<sup>1</sup> For the second cell, p-type [100] Si wafers were used as substrates. These wafers consisted of two silicon layers with different doping levels, *i.e.*, a low-doped (8 to 10  $\Omega\text{-cm}$ ) layer (8 to 10  $\mu\text{m}$  thick) grown epitaxially on a highly doped (0.008 to 0.02  $\Omega\text{-cm}$ ) Si substrate (500 to 550  $\mu\text{m}$  thick). The native oxide on the wafers was etched away in a 49% HF solution for about 5 s. The wafers were then loaded into a furnace and oxidized at 800°C in dry oxygen. Oxidation times varied between 30 min and 5 h to produce oxide layers of different thicknesses. Wafers with oxide layers of 50 to 100 Å, as determined by ellipsometry, were usually selected as the substrates. To fabricate the sandwich cells, a small amount of ZnOOEP powder was placed on an ITO surface, which was then heated to a temperature slightly higher than the melting point of ZnOOEP (*ca.* 180°C). Next, a piece of the oxidized Si wafer was placed on the top of the molten ZnOOEP drop, which was squeezed to produce a thin layer between the ITO and Si/SiO<sub>2</sub> surfaces. After cooling slowly from the isotropic liquid phase of ZnOOEP through the liquid crystalline phase to the solid at room temperature, sandwich cells of ITO/ZnOOEP/SiO<sub>2</sub>/Si were produced. The highly doped Si layer was always on the outside of the cells. The ZnOOEP layers were estimated to be 2 to 4  $\mu\text{m}$  thick by comparison of the maximum photocurrent with previous ITO/ZnOOEP/ITO cells. To produce thinner layers, the pressure between the Si and ITO was increased while the ZnOOEP was in a molten state.

The third cell, with a silicone polymer insulating layer, was used primarily for comparison to the Si/SiO<sub>2</sub> cell. In this case, ITO/ZnOOEP/ITO cells were separated so that one surface of the ZnOOEP film was free. Then, a well-polished Al rod (diameter,  $\sim 3$  mm; final polish with 50 nm gamma-alumina) coated with fresh silicone rubber was pushed against a ZnOOEP surface. The resulting cells have a structure of ITO/ZnOOEP/silicone/Al. The movement of the Al rod was controlled with an inchworm stepper (Burleigh) with a speed  $\geq 4$  nm/s. The silicone layer was pressed to the appropriate thickness ( $\sim 3 \mu\text{m}$ ) so that a clear photocapacitance was seen. Measurements were usually made after the silicone rubber was dry. ZnOOEP was synthesized as previously described.<sup>6,7</sup>

Instruments employed for capacitance measurements included a Tektronix 2440 500 MS/s digital oscilloscope operated at an input impedance of 1 M $\Omega$ , a Krohn-Hite Model 2400 AM/FM/phase lock function generator, an EG&G Princeton Applied Research Model 5206 two-phase lock-in analyzer, and a Keithley Instruments Model 590 C-V analyzer. In capacitance measurements, the applica-

tion of a constant bias to the cells in the range of  $-2$  to  $+2$  V had essentially no effect on the results. All data shown in this paper were obtained at 0 bias. A Xe lamp (Oriel) operated at 1250 W was used as the light source. A 420 nm cutoff filter and a 14 cm long circulating water bath were used to eliminate radiation in the UV and IR regions.

In cell charging and discharging experiments, the cell was biased with an EG&G PAR Model 173 potentiostat (auxiliary and reference leads shorted), and the bias was adjusted with an EG&G PAR Model 175 programmer. The current output was recorded with an oscilloscope or X-Y recorder. An argon ion laser (Coherent Innova 90) was used only for the ITO/ZnOOEP/ITO cells. The intensity was about 50 mW with a laser spot of about 375  $\mu\text{m}$  in diameter.

### Results

*ITO/ZnOOEP/ITO cell.*—The behavior generally followed that previously described for similar cells made with ZnODEP.<sup>1</sup> Briefly, such cells produce a photocurrent, even in the absence of a bias, by injection of electrons into the ITO electrode facing the light source. Under irradiation with a bias applied between the two ITO electrodes, larger photocurrents flow and a fraction of the current produces charges trapped within the ZnOOEP layer. The total amount of trapped charge depends upon the light intensity and bias voltage magnitude. The charge remains trapped in the dark, even under short-circuit conditions, for long times (days to months). This trapped charge is released, however, upon irradiation at short circuit, and this gives rise to a discharge photocurrent. Such trapping and detrapping occurs in an externally controllable manner superficially resembling the charging and discharging of a capacitor. Of interest in the application of such structures to storage of information is the amount of charge stored per unit area (or volume). Figure 1 shows the results of a typical charge/discharge experiment to measure the

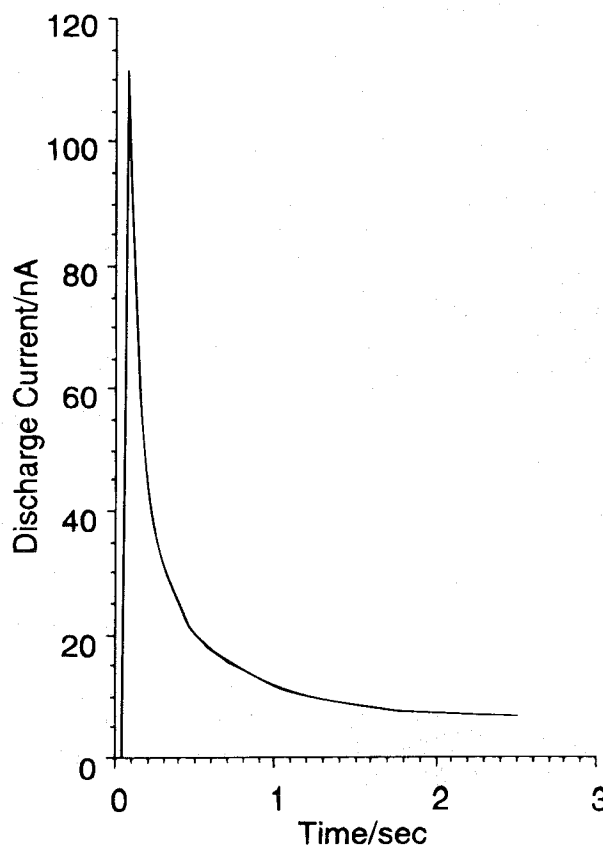


Fig. 1. Discharge current as a function of time for an ITO/ZnOOEP/ITO cell irradiated with a laser beam (375  $\mu\text{m}$  in diameter) at 514 nm under short-circuit conditions.

maximum effective storage density. The cell was irradiated with a 50 mW CW Ar laser (beam area  $1.1 \times 10^{-3} \text{ cm}^2$ ) with a 10 V bias for 10 s. The cell was discharged by irradiation with the same laser under short-circuit conditions, yielding the current-time curve in Fig. 1. The total charge passed during the 2.5 s discharge was 40 nC, yielding an effective storage charge density of  $36 \mu\text{C}/\text{cm}^2$ . As discussed below, this charge represents both trapped and photoinduced charges. The charge capacity of these cells varied with cell thickness, but a maximum effective storage density of at least  $30 \mu\text{C}/\text{cm}^2$  or about  $10^{18}$  charges/ $\text{cm}^3$  was attainable for 10 s charging times.

**ITO/ZnOOEP/SiO<sub>2</sub>/Si cell.**—The operation of this cell in the dark and under irradiation is shown in Fig. 2. Charges are stored in the dark by the application of an electric field (as with a conventional capacitor). Note that the dark resistivity of ZnOOEP is very high ( $\sim 10^{14} \Omega\text{-cm}$ , as estimated from the current-voltage curve), about the same as that of SiO<sub>2</sub> and Si<sub>3</sub>N<sub>4</sub>, so charges are stored in the dark only at the outermost interfaces. However, the ZnOOEP film becomes conductive under irradiation, and charges are then stored within the photoconductive layer and accumulate at the SiO<sub>2</sub> interface (Fig. 2B). Therefore, more charge is stored with irradiation because, with a decrease in ZnOOEP resistance, the electric field across the SiO<sub>2</sub> film becomes much larger with light than it does in the dark under the same external bias. Moreover, charges stored with irradiation do not disappear over time under short-circuit conditions in the dark, as discussed previously.<sup>1</sup>

As with the ITO/ZnOOEP cell, this phenomenon could provide a means of electro-optical information storage. Read-out of the data (charge) stored could be accomplished several ways, including photodischarge under short-circuit conditions.<sup>1</sup> As an optical data storage device, the size of a memory cell would be determined by the diameter of the write-read light spot. On the other hand, in the electrical write-read mode, the size of the individual memory cell is controlled by the area of the lithographically produced contact electrode.

Typical experimental charge and discharge cycles are shown in Fig. 3. In this case, a continuous square-wave potential ( $-0.4$  to  $+0.4$  V) was applied. Note that, in contrast to the ITO/ZnOOEP/ITO cell, no steady-state photocurrent was observed, even after the photocurrent was

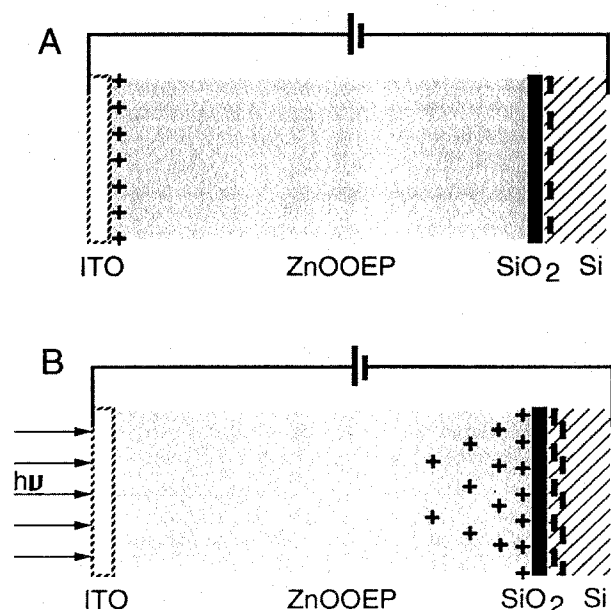


Fig. 2. Schematic diagram of the operational principles for charge storage in a photoconductive medium in the dark (A) and with irradiation (B).

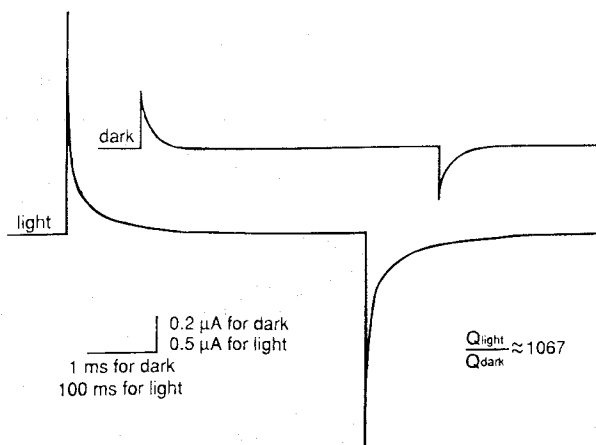


Fig. 3. Charge and discharge characteristics of the cell with and without irradiation. A continuous square-wave potential ( $-0.4$  to  $+0.4$  V) was applied.

amplified 1000 times. Since the oxide layer is relatively thick (50 to 100 Å), there is no tunneling current through the insulator. Breakdown causing irreversible permanent damage to the cells was found under high potential (e.g.,  $\geq 10$  V). This varied from sample to sample because of differences in the SiO<sub>2</sub> thickness. In a typical result for irradiation with a 0.12 cm<sup>2</sup> Xe lamp, at 0.4 V bias, the charge storage density was  $0.48 \mu\text{C}/\text{cm}^2$ .

The most remarkable feature in Fig. 3, however, is that the charge stored under irradiation is a thousand times that in the dark. An approximate equivalent circuit of the system would be that of three capacitors in series:  $C_{pc}$ , for the photoconducting layer;  $C_i$ , for the SiO<sub>2</sub> layer; and  $C_{sc}$ , for the space-charge layer in the Si semiconductor. The total measured capacitance,  $C$ , given in Eq. 1, would differ in the dark and under illumination

$$C^{-1} = C_{cp}^{-1} + C_i^{-1} + C_{sc}^{-1} \quad [1]$$

In the dark,  $C_i$  and  $C_{sc}$  would be much larger than  $C_{pc}$ , so  $C \approx C_{pc} \approx \epsilon_{pc}\epsilon_0 A/d_{pc}$ , where  $\epsilon_{pc}$  is the dielectric constant ( $\sim 2$ ),  $d_{pc}$  is the thickness ( $\sim 3$  to  $4 \mu\text{m}$ ) of the photoconducting layer, and  $\epsilon_0$  is the permittivity of free space. Under irradiation, the ZnOOEP becomes conductive, and  $C_{light} \approx C_i \approx \epsilon_i\epsilon_0 A/d_i$  with  $\epsilon_i \sim 4$  and  $d_i \sim 5$  to  $7.5 \text{ nm}$ . This yields  $C_{light}/C_{dark} \approx \epsilon_i d_{pc}/\epsilon_{pc} d_i \approx 800$  to  $1600$ ; the measured ratio for the cell in Fig. 3 was 1067, within this range.

Thus, this device can also be considered to be a light-controlled capacitor. Figure 4 shows the capacitance response to irradiation. The cell capacitance changed

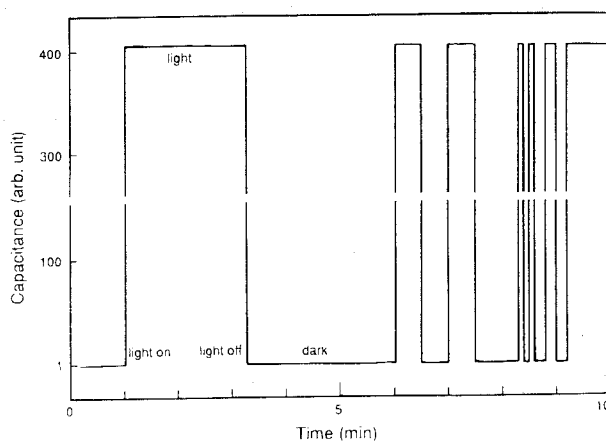


Fig. 4. Response of the ITO/ZnOOEP/SiO<sub>2</sub>/Si cell to irradiation as a function of time. A continuous sine-wave potential ( $-0.5$  to  $+0.5$  V) was applied with a frequency of 20 Hz.

markedly under irradiation. Note that the photocapacitance, which may vary from sample to sample due to differences in their physical geometries, was very stable and reproducible. When cells were irradiated continuously for 8 h with periodic checks of dark and photocapacitance (every 30 min), no changes were seen. In fact, ZnOOEP was found to be stable after two months of continuous irradiation for single-layer cells, and the number of reproducible charge-discharge cycles was well beyond 1.5 billion. A previous long-term stability test of ZnOOEP photocells led to the same conclusion.<sup>8</sup> The results in Fig. 4 were obtained at a frequency of 20 Hz. At high frequency, however, the ratio of light capacitance to dark capacitance decreased as shown in Fig. 5 because the time period was not sufficient to charge the cell fully in the configuration used here. A frequency dependence of the capacitance ratio (light/dark) was previously observed with photosensitive layers of the inorganic materials ZnS and CdS,<sup>9</sup> where a detailed analysis and simulation was given. However, the observed photocapacitance ratios of ZnS and CdS were much too small ( $C_l/C_d \approx 0.5$ ) to be of practical value, probably because the cell configuration involved a  $\sim 0.1$  mm thick mechanically pressed powder layer of the inorganic materials. For the relatively thick photoconductive ZnOOEP layers, the inner part of the material received little or no light flux and therefore had a higher resistivity. For ZnOOEP films, the light penetration depth depends on the wavelength.<sup>8</sup> The most strongly absorbed wavelength, at 380 nm, penetrates less than 0.6  $\mu\text{m}$  into the porphyrin layer, while at 586 nm, the penetration depth is  $\sim 2$   $\mu\text{m}$ . The thickness of the ITO/ZnOOEP/ITO cells ranged from 2 to 4  $\mu\text{m}$ . It was difficult to fabricate thinner cells with the technique used here, because the insulator films of  $\text{SiO}_2$  were often broken mechanically when a higher pressure was applied to the cells with the ZnOOEP in the molten state. When this happened, a larger steady-state short-circuit photocurrent was observed.

Several experiments were carried out to test if photoeffects in the Si substrate played any role. When a 700 nm cutoff filter was placed in front of the sample, so that the ZnOOEP film and  $\text{SiO}_2$  layer were transparent, the increase of capacitance under excitation of Si was negligible ( $<3\%$ ). When samples without silicon, *i.e.*, ITO/ZnOOEP/silicone/Al were employed, the results were similar to that with the Si/ $\text{SiO}_2$  substrate, suggesting again that Si served mainly as a back contact.

Figure 6 shows the dependence of capacitance ratio (light or dark) at a sine wave frequency of 1 kHz on the

light intensity (controlled with neutral density filters). The ratio increased with the intensity with no saturation reached at the maximum intensity used here. Variation of light intensity is a simple means of controlling the capacitance, which might be a useful feature in an electro-optical device.

## Discussion

To understand the operation of these cells, one must be aware that they are photovoltaic (*i.e.*, produce a photocurrent on irradiation with no bias) as well as photoconductive devices.<sup>1,8</sup> Upon irradiation of the ZnOOEP cells, photogenerated electrons are preferentially injected from the excited states of the porphyrin molecules into the irradiated ITO electrode, and photogenerated holes move into the porphyrin and are trapped there. As shown in Fig. 1, the ITO/ZnOOEP/ITO sandwich cells show effective charge storage capacities of at least  $30 \mu\text{C}/\text{cm}^2$  or  $10^{18}/\text{cm}^3$  (50 mW Ar laser, 10 V, 10 s). There are three possible mechanisms for charge storage within a solid organic thin film. (i) Charge is stored at the film surface (*i.e.*, two-dimensional storage) similar to that in a conventional capacitor with a dielectric layer like  $\text{SiO}_2$ . (ii) Charge is stored through a process of "persistent internal polarization."<sup>10-13</sup> Such polarization is attributed to a partial separation by the applied electric field of electron/hole pairs generated by the irradiation inside the photoconductive material and their localization in traps. (iii) Charge is stored through an electrochemical process, as in a battery. For example, with nigrosine paste sandwiched between silver electrodes, a discharge current of  $0.8 \text{ mA}/\text{cm}^2$  lasted for about 11 min, corresponding to a capacity of about  $0.5 \text{ C}/\text{cm}^2$ .<sup>14,15</sup> A combination of these mechanisms might be involved for the large charge storage capacity observed in ZnOOEP-based cells, although electrochemical (faradaic) changes appear unlikely, given the very large cycle life and the analogous behavior of ITO- and  $\text{SiO}_2$ -ZnOOEP junctions.

We call the charge actually measured on short-circuit discharge under irradiation,  $30 \mu\text{C}/\text{cm}^2$ , the effective charge,  $Q_{\text{eff}}$ .  $Q_{\text{eff}}$  is much larger than the actual trapped or stored charge,  $Q_s$ . The charge stored per unit area on a capacitor is given by

$$Q_s/Z = \epsilon\epsilon_0 V/d$$

or assuming  $\epsilon \approx 2$  for ZnOOEP and with  $\epsilon_0 = 8.85 \times 10^{-14} \text{ F}/\text{cm}$ , the field ( $V/d$ ) needed to produce a charge density of  $30 \mu\text{C}/\text{cm}^2$  would be  $1.7 \times 10^8 \text{ V}/\text{cm}$ . This is more

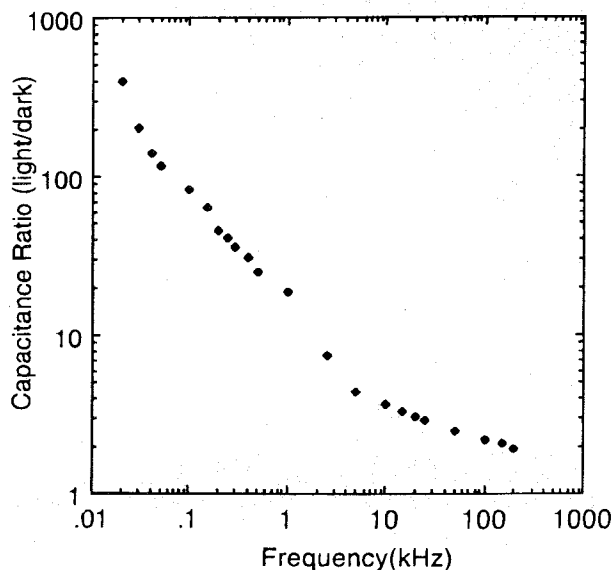


Fig. 5. Dependence of capacitance ratio (light/dark) on the frequency. A continuous sine-wave potential ( $-0.5$  to  $+0.5$  V) was applied.

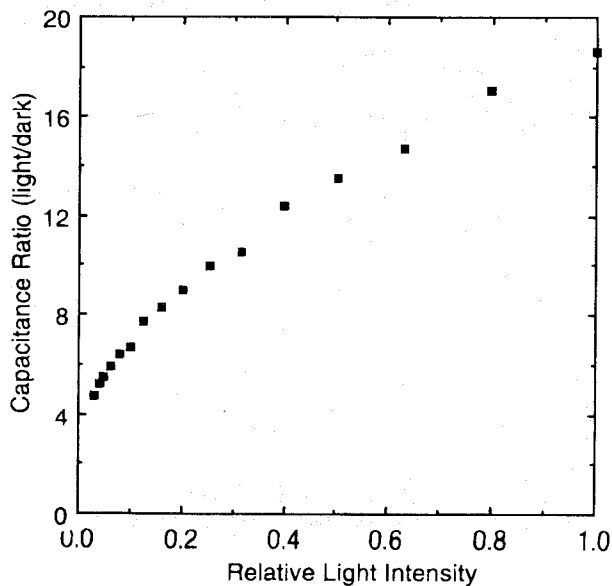


Fig. 6. Dependence of capacitance ratio (light/dark) on the light intensity. A continuous sine-wave potential ( $-0.5$  to  $+0.5$  V) was applied with a frequency of 1 kHz.

than an order of magnitude larger than the field that can be sustained without breakdown by SiO<sub>2</sub> and almost certainly that for breakdown of ZnOOEP. Thus the discharge current and the measured effective charge obtained by integration of the current must involve two components, one that is due to the actual trapped charge and a second that is due to a photocurrent induced by the trapped charge, *i.e.*

$$Q_{\text{eff}} = Q_s + Q_{\text{ph}}$$

where  $Q_{\text{ph}}$  is the integrated photocurrent generated by the light. We propose that the local electric field produced by trapped charge assists in the dissociation of an exciton into an electron/hole pair thus giving rise to a larger photocurrent than would be observed in the absence of such lattice charge. This is consistent with previous findings that an exciton in an inorganic material can dissociate in the electric field produced by an ionized impurity or in the space-charge created at the surface.<sup>16</sup> It also explains an earlier finding<sup>10</sup> that the total amount of charge needed to cancel an "induced polarization" was larger than the polarization charge. It is also consistent with the very high density charge trapping ( $10^{15}$  to  $10^{18}$  charges/cm<sup>3</sup>) previously reported for organic films.<sup>14,17</sup> This effect allows a significant level of amplification of the current resulting from a small amount of trapped charge and may be important in high-density memory devices.

A high charge density is desirable in data storage devices. Indeed, with currently available MIS materials, the memory cells cannot be reduced much further in size and still maintain the minimum storage capacity in dynamic or static random access memories. This limitation can be overcome to a limited degree<sup>2</sup> by fabricating more complicated three-dimensional structures, such as the trench capacitor and "stacked" capacitor, which increases the surface area to increase the total charge storage capacity.<sup>2,5</sup>

While charge storage density is the determining factor for some high density memory devices, such as dynamic and static random access memory, it is less critical for nonvolatile memory where the rewrite ability is a primary concern for the present. Charge trapping in thin films has long been studied as a means of information storage, for example, in MIOS structures like metal/Si<sub>3</sub>N<sub>4</sub>/SiO<sub>2</sub>/Si, which have been proposed as electrically erasable and programmable read-only memories.<sup>18</sup> In this case, under a high voltage pulse, charges tunnel from the substrate Si through the SiO<sub>2</sub> (a few tens of angstroms thick) and are trapped in the Si<sub>3</sub>N<sub>4</sub> film. The charges can be removed with a high voltage pulse of opposite sign. The reversibility of this system, however, is poor, *i.e.*, the number of charge-discharge cycles is limited. A fatigue phenomenon, caused in part by the pulsed high electric field which forces the current through the SiO<sub>2</sub>, produces degradation

of the insulator layer.<sup>19</sup> This problem does not exist in our system where photoinduced trapping and detrapping occur under low bias.

### Acknowledgments

We thank Dr. B. A. Gregg for his synthesis of the ZnOOEP and Dr. M. A. Fox for valuable discussions. The support of this work initially by the Texas Advanced Research Program and by a grant from Texas Instruments is gratefully acknowledged.

Manuscript submitted July 19, 1995; revised manuscript received Feb. 26, 1996.

*The University of Texas at Austin assisted in meeting the publication costs of this article.*

### REFERENCES

1. C.-Y. Liu, H.-L. Pan, M. A. Fox, and A. J. Bard, *Science*, **261**, 897 (1993).
2. A. F. Tasch and L. H. Parker, *Proc. IEEE*, **77**, 374 (1989).
3. L. H. Parker and A. F. Tasch, *IEEE Circuits Devices Mag.*, **17** (1990).
4. S. M. Sze, *Physics of Semiconductor Devices*, 2nd ed., John Wiley & Sons, Inc., New York (1981).
5. B. Prince, *Semiconductor Memories*, 2nd ed., John Wiley & Sons, Inc., New York (1991).
6. B. A. Gregg, M. A. Fox, and A. J. Bard, *J. Chem. Soc., Chem. Commun.*, 1143 (1987).
7. B. A. Gregg, M. A. Fox, and A. J. Bard, *J. Am. Chem. Soc.*, **111**, 3024 (1989).
8. B. A. Gregg, M. A. Fox, and A. J. Bard, *J. Phys. Chem.*, **94**, 1586 (1990).
9. S. Kronenberg and C. A. Accardo, *Phys. Rev.*, **101**, 989 (1956).
10. H. Kallmann and B. Rosenberg, *ibid.*, **97**, 1596 (1955).
11. J. R. Freeman, H. P. Kallmann, and M. Silver, *Rev. Mod. Phys.*, **33**, 553 (1961).
12. V. M. Fridkin and I. S. Zheludev, *Photoelectrets and the Electrophotographic Process*, Consultants Bureau, New York (1961).
13. G. M. Sessler, *Electrets*, Springer-Verlag, New York (1980).
14. H. Meier, *Organic Semiconductors*, Verlag Chemie, Weinheim (1974).
15. K. J. Euler, G. Ryhiner, and P. Scholz, *Z. Angew. Phys.*, **24**, 32 (1967).
16. N. V. Joshi, *Photoconductivity: Art, Science, and Technology*, p. 130, Marcel Dekker, Inc., New York (1990).
17. J. Simon and J.-J. André, *Molecular Semiconductors: Photoelectrical Properties and Solar Cells*, Springer-Verlag, Berlin (1985).
18. J. R. Cricchi, J. S. Britton, and L. G. Ottobre, *ISSCC Digest of Technical Papers*, p. 98 (1972).
19. J. J. Chang, *Proc. IEEE*, **64**, 1039 (1976).